Determination of Interface Heat-Transfer Coefficients for Permanent-Mold Casting of Ti-6Al-4V

P.A. KOBRYN and S.L. SEMIATIN

Interface heat-transfer coefficients (h_0) for permanent-mold casting (PMC) of Ti-6Al-4V were established as a function of casting surface temperature using a calibration-curve technique. Because mold geometry has a strong effect on h_0, values were determined for both of the two limiting interface types, "shrink-off" and "shrink-on." For this purpose, casting experiments with instrumented molds were performed for cylinder- and pipe-shaped castings. The measured temperature transients were used in conjunction with two-dimensional (2-D) axisymmetric finite-element method (FEM) simulations to determine $h_0(T)$. For the shrink-off interface type, h_0 was found to decrease linearly from 2000 to 1500 W/m^2 K between the liquidus and the solidus, from 1500 to 325 W/m^2 K between the solidus and the gap-formation temperature, and at a rate of 0.3 W/m^2 K/K thereafter. For the shrink-on interface type, h_0 was found to *increase* linearly from 2000 to 2500 W/m^2 K between the liquidus and the solidus temperatures, from 2500 to 5000 W/m^2 K between the solidus and the gap-formation temperature, and to remain constant thereafter. The shrink-on values were up to 100 times the shrink-off values, indicating the importance of accounting for the interface geometry in FEM simulations of this process. The FEM-predicted casting and mold temperatures were found to be insensitive to certain changes in the h_0 values and sensitive to others. A comparison to published h_0 values for PMC of aluminum alloys showed some similarities and some differences.

I. INTRODUCTION AND BACKGROUND

PERMANENT-MOLD casting (PMC) is a well-known casting technique in which a component is made by pouring liquid metal into a reusable metal mold. The method is frequently used for the casting of aluminum alloys. In this case, the molds are typically made of steel. Advantages over sand or investment casting include the elimination of processing steps (because the mold can be reused) and the refinement of as-cast grain size, a result of faster cooling.

Recently, the application of PMC to the casting of titanium alloys has been investigated.[1] Ti PMC provides a means of producing relatively complex parts with close tolerances and finer grain sizes. In comparison to investment casting of titanium, Ti PMC requires fewer processing steps, greatly reduces the size of the alpha case, and eliminates the risk of ceramic inclusions. Therefore, the process is extremely attractive to the aerospace industry.

Process simulation *via* finite-element-method (FEM) solidification modeling is particularly critical to the development and eventual implementation of Ti PMC, as it can be used in lieu of expensive casting experiments for both process development and process design. Hence, much research on Ti PMC has focused on developing such modeling capabilities. Determination of interface heat-transfer coefficients is a critical step in this development. The interface heat-transfer coefficient (h_0) is used to quantify the resistance of an interface to the transfer of heat. It is defined by the equation $q = h_0(T_2 - T_1)$, in which T_1 and T_2 are the temperatures on either side of the interface, and q is the heat flux per unit area across the interface.[2] Although no h_0 values have been determined for Ti PMC, several researchers have studied interface heat transfer during the metal-mold casting of aluminum and iron alloys.[3–6]

Nishida and Matsubara[3] studied the effect of pressure on h_0 for casting of aluminum in a cylindrical carbon-steel mold. The resulting maximum h_0 values varied by more than an order of magnitude from an applied pressure of 0 to 100 MPa. Nishida *et al.*[4] determined h_0 for pure aluminum and Al-13.2Si alloys cast in graphite-coated molds of either a cylindrical or flat geometry. They found that the level of mold constraint had a large effect on h_0 while alloy composition had only a small effect. Sully[5] studied the effect of casting size, casting alloy, mold material, and mold geometry on h_0. From these observations, Sully concluded that (1) geometry affects h_0 significantly while the mold material and the casting alloy have only a small effect on it; (2) casting size controls the temporal variation of h_0; and (3) casting surface temperature has a large effect on h_0, but the mold surface temperature does not. Kim and Lee[6] studied the variation of h_0 with time, mold-coating type, and casting alloy for tube-shaped (*i.e.*, hollow cylinder or pipe) aluminum-alloy castings. Their results showed a marked difference in the magnitude and shape of $h_0(t)$ for the outer and inner mold-casting interfaces and a dependence on alloy solidification type (*i.e.*, solid-shell-forming *vs* mushy (or coherent-dendrite-network-forming)).

These previous measurements of h_0 reveal a wide range of values for different casting conditions (Table I). The maximum h_0 values were of the order of 50 kW/m^2 K for an applied casting-mold interface pressure of 100 MPa, while the typical maximum values in real castings (*i.e.*, without an externally applied pressure) ranged from 1.5 to 4.5 kW/m^2 K for outer mold-casting interfaces and from 10 to 100 kW/m^2 K for inner mold-casting interfaces. The minimum values were on the order of 0.10 kW/m^2 K (for an interface

P.A. KOBRYN, Materials Research Engineer, and S.L. SEMIATIN, Senior Scientist, Materials Processing/Processing Science, are with the Air Force Research Laboratory, Materials and Manufacturing Directorate, AFRL/MLLMP, Wright-Patterson Air Force Base, OH 45433-7817.

Manuscript submitted May 30, 2000.

Table I. Published Values of h_0 for Metal-Mold Casting Processes

Source	Maximum h_0 (kW/m^2 K)	Minimum h_0 (kW/m^2 K)	Casting Alloy	Mold Material	Contact Condition/ Geometry
Nishida and Matsubara[3]	~50	N/A	various Al alloys	carbon steel	100 MPa/cylinder
Nishida and Matsubara	~5.0	N/A	various Al alloys	carbon steel	1 MPa/cylinder
Nishida and Matsubara	~2.5	<0.4	various Al alloys	carbon steel	0 MPa/cylinder
Nishida *et al.*[4]	3.25	~0.25	various Al alloys	graphite-coated	0 MPa/cylinder
Nishida *et al.*	4.5	~0.1	various Al alloys	graphite-coated	0 MPa/plate
Sully[5]	2.75	~0.5	gray iron	modified steel	0 MPa/plate
Kim and Lee	~2.9	~0.15	various Al alloys	coated steel	0 MPa/pipe, outer mold
Kim and Lee[6]	~100	~0.25	various Al alloys	coated steel	0 MPa/pipe, inner mold

gap size of approximately 0.25 mm) and 0.25 kW/m^2 K, respectively.

The present work was undertaken to determine the interface heat-transfer coefficient during Ti PMC and, thus, to obtain data for FEM solidification models of the process. Published results for aluminum- and iron-alloy casting were used to guide the investigation. The technique applied here, an iterative calibration-curve method, involved the determination of interface heat-transfer coefficients using a combination of casting experiments with instrumented molds and FEM solidification modeling. The applicability of the resulting h_0 data to prototype-production castings was demonstrated in a parallel effort.[7]

II. APPROACH

A. *Materials*

The materials used in this investigation consisted of Ti-6Al-4V melt stock and H13 tool steel for the molds and mold cores. The Ti-6Al-4V had a composition (in wt pct) of 6.52 aluminum, 4.18 vanadium, 0.2 iron, 0.0298 carbon, 0.221 oxygen, 0.012 nitrogen, 23.5 ppm hydrogen, and balance titanium. The H13 tool steel was used to make (reusable) cylinder molds and (sacrificial) cylindrical mold cores. The cylinder molds were 230-mm tall and had a wall thickness of 25 mm and an inner diameter of 51 or 57 mm. The cores were 230-mm tall with a 1-deg taper from top to bottom and had a midheight diameter of either 25 or 32 mm.

B. *Casting Experiments*

Casting experiments were performed to collect data for determining values of the interface heat-transfer coefficient during Ti PMC. Two casting shapes were chosen to obtain lower and upper bounds for h_0 based on the contact condition at the casting-mold interface (*i.e.*, "shrink off" or "shrink on" interface type). Solid-cylinder castings (which shrink away from the mold wall during casting) were used to establish shrink-off h_0 values, while hollow cylinders (*i.e.*, pipes, which shrink onto the mold core during casting) were used to establish shrink-on h_0 values.

For the shrink-off h_0 experiments, the 51-mm-diameter mold was used. Thermocouples were placed in both the mold and the casting. Two 1.5-mm-diameter exposed-bead and two 0.79-mm-diameter coaxial type-K thermocouples were placed radially at each of two different depths in the mold (6.4 and 0.64 mm from the mold cavity), and one 1.5-mm-diameter exposed-bead type-B thermocouple was

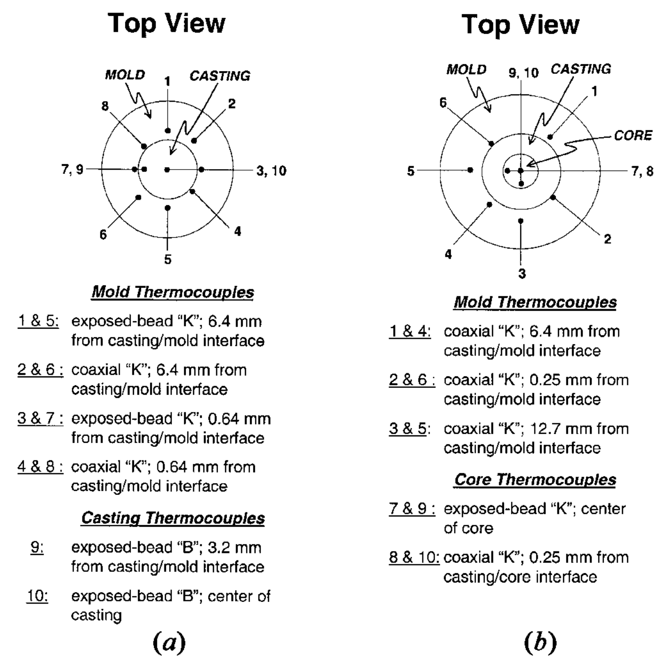

Fig. 1—Mold schematic illustrations showing thermocouple types and locations for casting experiments: (*a*) shrink-off mold and (*b*) shrink-on mold.

placed at each of two different depths in the casting (3.2 mm from the mold wall and at the center of the casting) (Figure 1(a)).

For the shrink-on h_0 experiments, the cores were placed in the 57-mm-diameter cylinder mold. Thermocouples were placed in both the outer mold and the mold cores. Two 0.79-mm-diameter coaxial type-K thermocouples were placed radially at each of three different depths in the mold (0.25, 6.4, and 12.7 mm from the mold cavity) and one depth in the core (0.25 mm from the mold cavity); two 1.5-mm-diameter exposed-bead type-K thermocouples were placed radially at the center of the core (Figure 1(b)). The thermocouples in the core were protected by molybdenum tubes, which were countersunk into the core to prevent molten Ti-6Al-4V from entering.

Casting was performed in a vacuum-induction-melting (VIM) chamber using specially fabricated MONOSHELL* melting crucibles from Howmet Corporation. The temperature of the Ti-6Al-4V during melting was monitored using a two-color infrared (IR) pyrometer. The thermocouples were

*MONOSHELL is a trademark of Howmet Corporation, Whitehall, MI.

connected to a PC-based data-acquisition system and temperatures were recorded at a rate of 50 Hz for the first 30 seconds and 10 Hz thereafter. Casting was done by tilting the crucible and allowing the molten Ti-6Al-4V to flow into the mold from the top. Six castings were made with the 51-mm-diameter shrink-off mold configuration while two castings were made with each of the two shrink-on mold configurations. Additional castings into the 57-mm-diameter mold (without or with cores) were made to establish the validity of the h_0s determined from the initial castings.

C. h_0 *Determination*

The thermocouple data were used in conjunction with FEM simulation results to determine heat-transfer coefficients for the shrink-off and shrink-on casting geometries using an iterative calibration-curve method. The following procedure was used:

(1) The thermocouple data were prepared for comparison to FEM results.
(2) The form of the $h_0(T)$ curve was guessed.
(3) Two-dimensional axisymmetric FEM simulations of the different casting geometries were set up and conducted.
(4) Calibration curves were generated from the FEM results and compared to the experimental temperature *vs* time measurements.
(5) Steps 3 and 4 were repeated using different values of $h_0(T)$ until a suitable agreement between the simulated and measured temperature profiles was obtained.

1. *Thermocouple data preparation*

The thermocouple data were collected, imported into a spreadsheet, averaged, and smoothed. In general, a representative pour was chosen for each casting configuration for the determination of h_0.

2. *Selection of a general* h_0 *curve*

Because h_0 is usually a strong function of temperature/time, a general form of the h_0 curve had to be selected. This form was chosen as follows based on the expected changes in the interface contact condition as solidification progressed. Initially, the Ti-6Al-4V casting is liquid, and the contact between the casting and the mold is very good; h_0 is, therefore, very high. As the Ti-6Al-4V cools, the viscosity and surface tension change, and the contact between the casting and the mold degenerates slightly, causing h_0 to decrease slightly. Once solidification begins, a solid skin forms at the interface, and interfacial contact occurs only at asperities. As solidification proceeds, the solid skin grows and becomes stronger. From this point on, h_0 becomes strongly geometry dependent. In the shrink-off case, once the skin is strong enough to resist deformation (due to the head of liquid Ti-6Al-4V), it begins to shrink away from the mold and a gap forms at the interface. As the gap forms, the method of interface heat transfer changes from conduction to radiation, and h_0 drops dramatically.[8] Subsequently, h_0 is controlled by the emissivity of the surface of the casting, the temperature of the casting, and the mold on either side of the interface. In the shrink-on case, the casting shrinks and the core expands as heat is conducted from the casting to the core. Hence, contact between the casting and the core improves, and, correspondingly, h_0 increases. The value of h_0 is then controlled by the contact pressure at the interface, and it continues to increase with pressure until a limit is reached and h_0 remains constant.[9,10]

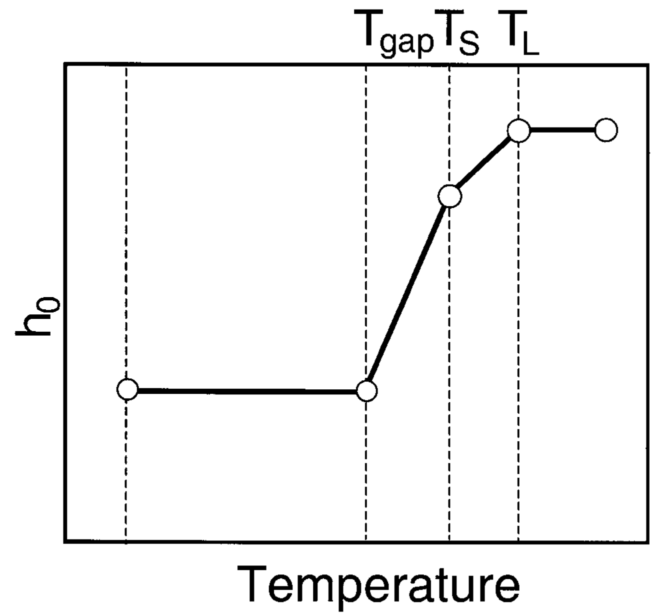

Fig. 2—Example $h_0(T)$ curve for the shrink-off interface type.

To generate an interface-heat-transfer-coefficient curve based on the above description, h_0 was assumed to be a function of casting surface temperature (Figure 2). The temperature of the surface of the casting was selected as the independent variable instead of time to eliminate any dependence on the size of the casting and to provide a correlation between the values of h_0 and the physical state of the interface. To simplify the $h_0(T)$ curve, temperatures at which sudden changes in the slope of the curve occurred were chosen, and the shape of the curve between these temperatures was assumed to be linear. Specifically, solidification was assumed to start at the liquidus temperature T_L (1654 °C) and end at the solidus temperature T_S (1620 °C); gap formation (in the shrink-off case) was assumed to occur at a temperature T_{gap} between 1600 °C and 1450 °C. Initial estimates of h_0 at and above the liquidus and at the solidus were made based on published data for aluminum casting, while an initial estimate of the gap-formation temperature was made based on the thermocouple measurements themselves. The radiation heat-transfer coefficient at selected post-gap-formation temperatures was estimated from the emissivity of the Ti-6Al-4V (~0.25) and the temperatures of the mold and casting at the interface. In the shrink-on case, the contact pressure at the interface was assumed to cause a linear increase in h_0 between the solidus and the previously determined shrink-off gap-formation temperature, after which the coefficient was assumed to remain constant.

3. *FEM calibration curves*

Axisymmetric (two-dimensional) (2-D) FEM models of all of the casting geometries were generated using the PROCAST* solidification-modeling package.[11] Thermal-only

*PROCAST is a trademark of UES Software, Inc., Dayton, OH.

simulations were performed to solve the transient nonlinear heat conduction equation and heat transfer across the casting-mold interface was modeled using PROCAST's coincident-node technique.[11] Input to the program included the thermophysical properties of the casting and mold materials as a function of temperature,[12,13] the experimentally determined initial temperatures of the molten Ti-6Al-4V and the steel molds, and the initial estimates of h_0 at selected temperatures. The external mold boundary condition was specified as a simple radiation heat-flux boundary condition. The molds were assumed to be instantaneously filled with molten Ti-6Al-4V at the start of the simulations.

The 51-mm-diameter shrink-off casting simulation was performed first. The predicted temperature transients at nodes corresponding to thermocouple locations were plotted to form calibration curves for heat-transfer-coefficient determination. The measured thermocouple data were then plotted, and the agreement between the simulated and measured temperature histories was determined. If the match was unsatisfactory, the initial $h_0(T)$ curve was modified manually, and the simulation was run again. This process was repeated until a reasonable agreement was obtained between the calibration curves from a single simulation and the measured temperature traces. Once the shrink-off coefficients were determined, the results were used for the *outer interface* in the simulations for the shrink-on $h_0(T)$ values. The shrink-on values were then determined in a similar manner.

D. *Sensitivity Analysis and Comparison to Published Data for Aluminum Alloys*

The sensitivity of the FEM-predicted mold and core temperatures to errors in the $h_0(T)$ values was assessed by performing additional 2-D simulations of the 51-mm-diameter shrink-off casting and the 32-mm-internal-diameter shrink-on casting. The effects of a 50 pct increase in the values of h_0 at all temperatures and a 50, 100, and 1000 pct increase in the value of h_0 at temperatures at and above the liquidus were assessed for both castings, while the effect of an increase in the final shrink-on h_0 value of 50, 100, and 1000 pct was assessed for the shrink-on casting.

In addition, the h_0 values determined in the present work were compared to published aluminum-alloy h_0 data by converting to $h_0(t)$ curves and plotting them on the same axes as the aluminum-alloy data. Differences in $h_0(t)$ were interpreted in terms of the difference in the two casting processes.

III. RESULTS AND DISCUSSION

The principal results of this investigation comprised the shrink-off and shrink-on $h_0(T)$ curves determined from thermocouple measurements, the validation of the $h_0(T)$ curves for similarly shaped castings, an analysis of the sensitivity of the predicted mold temperatures to changes in the $h_0(T)$ curves, and a comparison of the h_0s for Ti PMC to published values for PMC of aluminum alloys.

A. *Shrink-Off Results*

1. *Temperature measurements for 51-mm-diameter mold*

Accurate temperature transients could not be measured in the castings (because thermocouples dissolve in molten Ti-6Al-4V); thus, only thermocouple data from the molds were

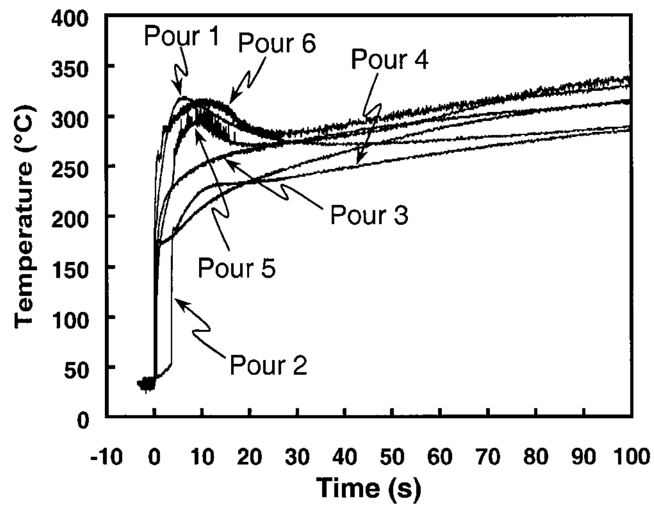

(*a*)

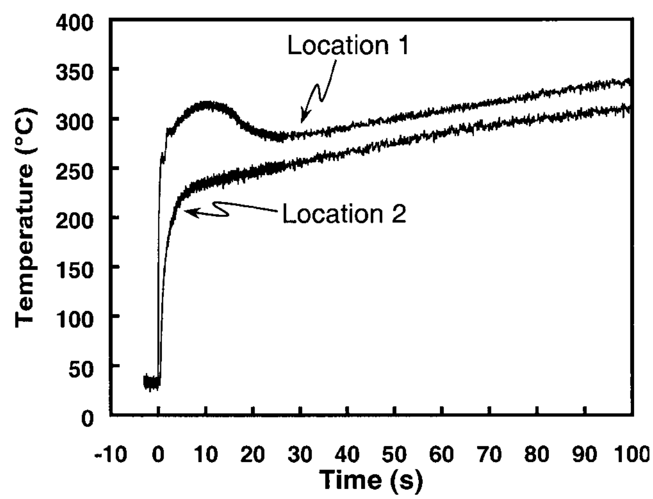

(*b*)

Fig. 3—Thermocouple data from the 51-mm-diameter mold illustrating (*a*) pour-to-pour variability and (*b*) location-to-location variability. All measurements were made 0.64 mm from the surface of the mold.

used to determine $h_0(T)$. Both pour-to-pour and location-to-location variability were observed in these data (Figure 3). While the pour-to-pour variability was random, the location-to-location variability was systematic. The principal cause of the pour-to-pour variability of a specific thermocouple result was determined to be slight differences in the way in which the molten Ti-6Al-4V flowed into the mold (as evidenced by videos of each pour), while the principal cause of the location-to-location variability within a single pour was determined to be the way in which the molten Ti-6Al-4V filled the mold by flowing down one side and up the other (as evidenced by the results of a three-dimensional simulation of the tilt-pouring operation). The instantaneous temperature difference for a single thermocouple over six pours ranged from 100 °C during the initial transient to 50 °C during the later stages of casting, while the instantaneous temperature difference between two thermocouples (located at the same depth) for a given pour ranged from over 100 °C during the initial transient to less than 25 °C during the later stages of casting. Both types of variability were addressed before the calibration-curve method was applied.

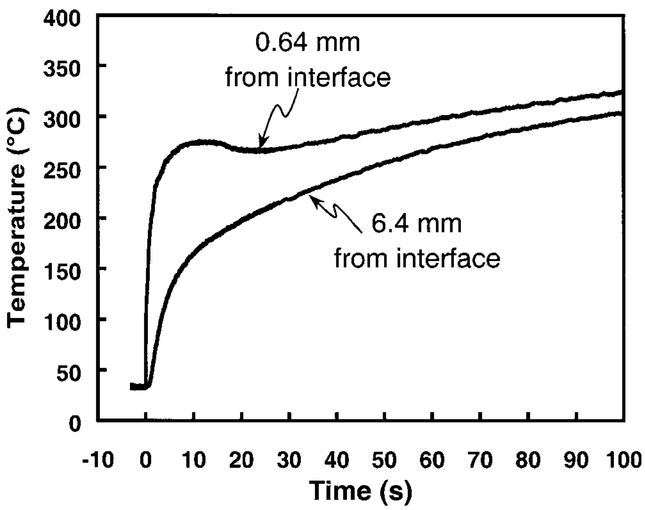

Fig. 4—Averaged data for thermocouples at depths of 0.64 and 6.4 mm from the interface for a representative pour into the 51-mm-diameter mold, illustrating the important features to be matched by FEM simulations.

Because the pour that exhibited the highest measured mold temperatures was most likely the one for which the effect of mold filling was the least (and because mold filling was *not* modeled), data from this pour were used for the determination of the shrink-off h_0 values. Furthermore, because the two same-depth thermocouples on opposite sides of the mold would have experienced the extremes of local temperature due to the systematic difference in the time at which the flowing melt reached the two locations, an average of the data from these two thermocouples was used for h_0 determination.

Average thermocouple data from the chosen pour illustrated the key features that had to be matched by the simulated mold temperature transients (Figure 4). These features included the initial heating rate at both thermocouple depths, the time and size of the initial peak at the 0.64-mm-depth, the time of the change in slope at the 6.4-mm-depth, and the subsequent heating and cooling rates and peak temperatures at both depths.

2. *Calibration curves and shrink-off h_0 values*

The features of the measured mold temperature-transient curves were matched very well when a $h_0(T)$ curve determined by the method described in section III.A (Figure 5(a)) was used in a 2-D simulation (Figure 5(b)). The maximum instantaneous temperature difference between the measured and predicted curves was less than 10 °C. When the Ti-6Al-4V was liquid, the value of h_0 was 2000 W/m^2 K. As solidification proceeded, h_0 dropped linearly from 2000 to 1500 W/m^2 K. As the solid skin separated from the mold wall (thereby forming a gap at the interface), h_0 dropped from 1500 to 325 W/m^2 K. After the gap formed, h_0 decreased linearly with decreasing casting surface temperature at a rate of approximately 0.3 W/m^2 K^2.

3. *Shrink-off h_0 validation*

Thermocouple data collected from two pours into the 57-mm-diameter mold and accompanying FEM-simulation predictions established the accuracy of the h_0 values determined from the trials with the 51-mm-diameter mold. As for the 51-mm-diameter casting trials, the pour with the higher measured mold temperatures was selected, and data from thermocouples at the same depth were averaged. FEM-predicted temperature transients (made with the $h_0(T)$ in Figure 5(a)) were compared to the average measured temperature transients for the three thermocouple depths; the resulting comparison was reasonable (Figure 6). The initial slopes and the times at which the slopes of the curves changed were predicted accurately, while the instantaneous temperature values were overpredicted by 50 °C or less. The only exception was for the temperatures at the 6.4-mm-depth, in which case the overprediction was more than 50 °C. However, upon comparison to data from the other thermocouples, an error in the thermocouple data from this depth was evident (Figure 6); the measured temperatures were consistently lower than they should have been. Hence, a quantitative comparison of the temperatures was not made, and only the broad shapes of the measured and predicted curves were compared at this location.

Because the difference between the measured and predicted data was within the expected range of pour-to-pour variability (based on data from the 51-mm-diameter mold),

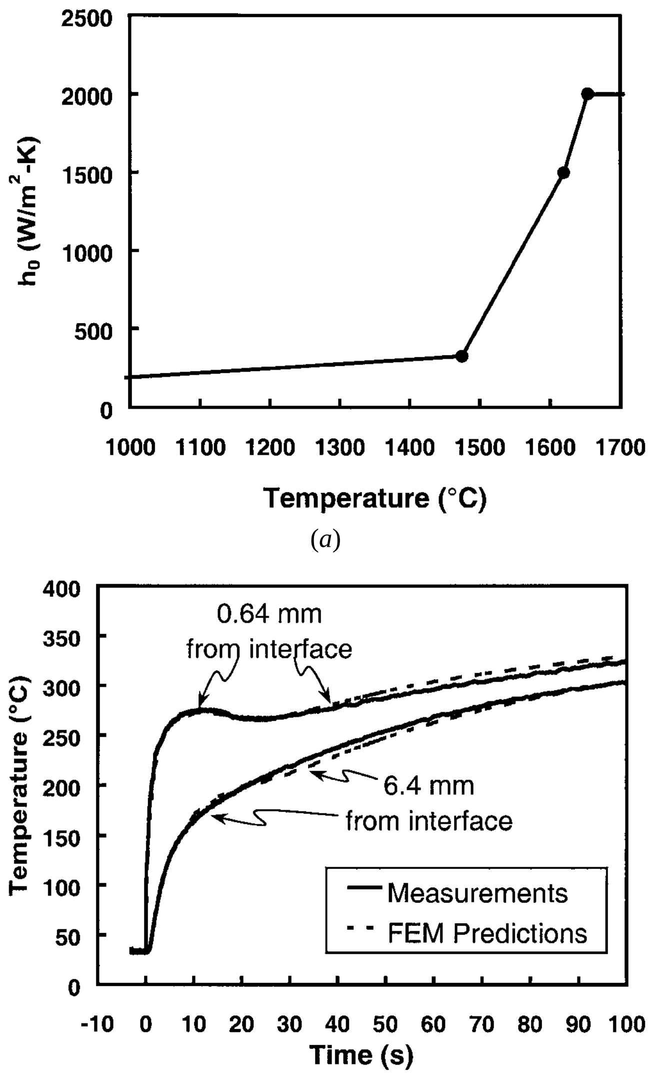

(*a*)

(*b*)

Fig. 5—Calibration-curve results for shrink-off casting conditions: (*a*) the $h_0(T)$ curve and (*b*) comparison of measured and FEM-predicted mold-temperature transients.

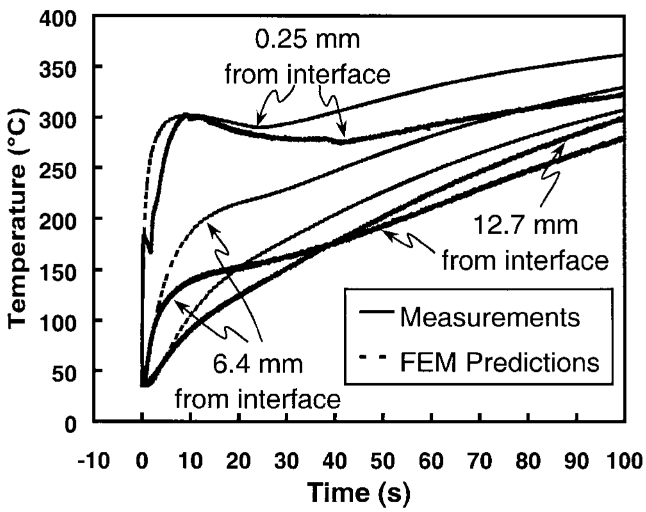

Fig. 6—Comparison of the (average) measured temperatures for three thermocouple locations in a 57-mm-diameter mold and those predicted by an FEM simulation using the $h_0(T)$ curve in Fig. 5(a).

the $h_0(T)$ curve determined from the 51-mm-diameter-mold trials was deemed to be generally applicable for shrink-off conditions.

B. *Shrink-On h_0 Results*

1. *Temperature measurements*

Thermocouple data were collected for two pours into the 57-mm-diameter mold with either the 32-mm-diameter core or the 25-mm-diameter core. These data showed less consistency than the shrink-off data because mold filling was less smooth (due to the presence of the cores and the molybdenum protection tubes). In contrast to the shrink-off data, both the pour-to-pour *and* location-to-location variability were random in this case (Figure 7). In addition to the increased and unpredictable variability, the data indicated that one or more thermocouples either had separated from the mold or had failed during casting. Therefore, it was not possible to choose a single pour and average the data from the two thermocouples at the same depth within that pour

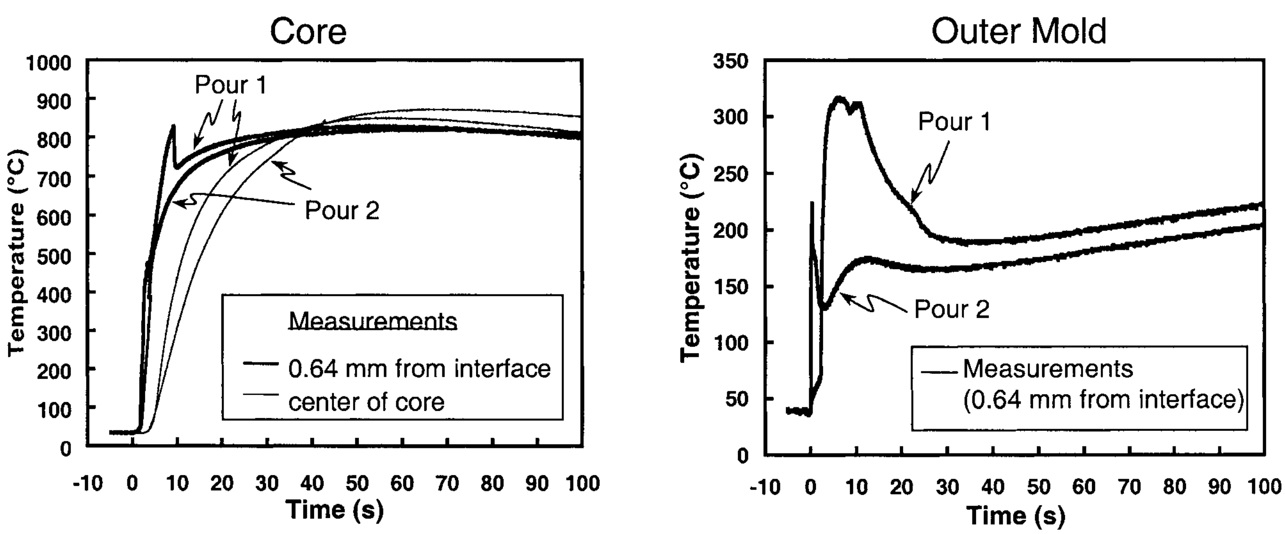

(*a*)

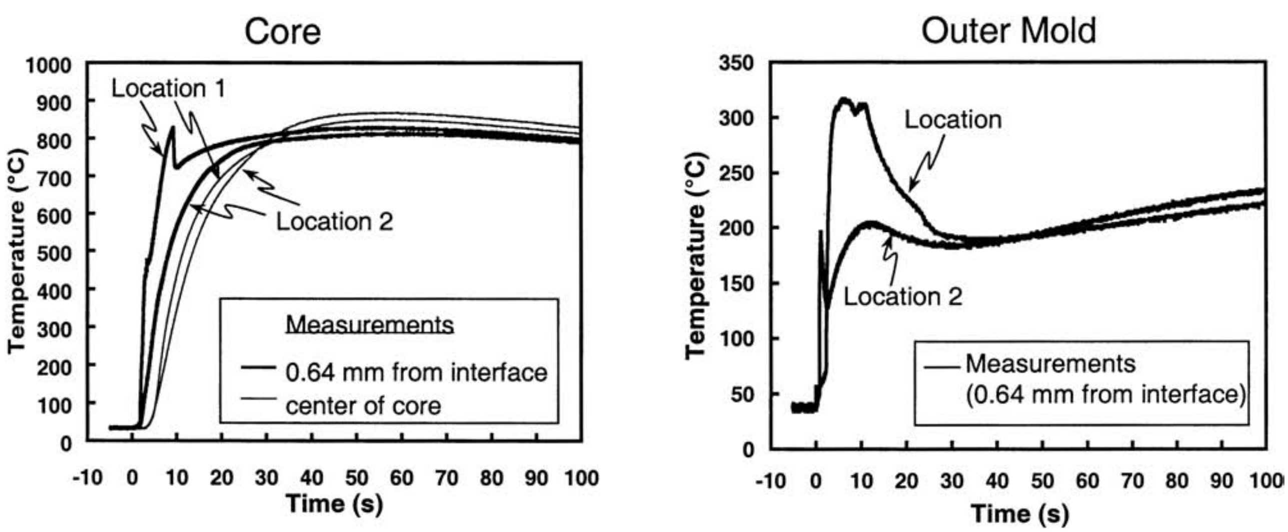

(*b*)

Fig. 7—Measured temperature transients for casting with a 57-mm-diameter mold and a 25-mm-diameter core illustrating (*a*) pour-to-pour variability and (*b*) location-to-location variability.

for comparison to simulated temperature transients. Instead, data from both pours were used. Data from the two same-depth thermocouples within a single pour were averaged when feasible; otherwise, data from single thermocouples were used.

Another complication with the shrink-on thermocouple data was the apparently anomalous difference between the peak temperatures near the surface and those in the center of the cores (Figure 7). In all cases, the measured peak temperature at the center of the core was significantly higher than that near its surface. This behavior, while not impossible, is not likely to have actually occurred; thus an explanation was sought. The most likely explanation was that the near-surface thermocouples separated from the cores while the center thermocouples maintained good contact. Some of the near-surface data showed evidence of a sudden loss of contact with the core, while none of the center data showed such indications (Figure 7), thereby giving credence to this hypothesis. Hence, only the shape and/or the initial heating rate data were used for the near-surface core locations in determining shrink-on heat-transfer characteristics.

2. *Calibration curves for 32-mm-diameter core*

The main features of the measured *core* temperature-transient curves were matched very well when an $h_0(T)$ curve determined using the method described in section III.A (Figure 8(a)) was used in conjunction with the shrink-off $h_0(T)$ curve in a 2-D FEM simulation (Figure 8(b)). The maximum instantaneous temperature difference between the measured and predicted curves at the center of the core was less than 50 °C, and both the initial heating rate and the shape of the predicted near-surface curve matched those of the measured curves. As in the shrink-off case, when the Ti-6Al-4V was liquid, the value of h_0 at the casting-core interface was 2000 W/m^2 K. Thereafter, the similarities between the shrink-off and shrink-on curves ceased. Instead of decreasing as solidification proceeded, h_0 *increased* linearly from 2000 to 2500 W/m^2 K. As the solid skin shrunk onto the core (thereby increasing the contact pressure at the interface), h_0 *increased further* from 2500 to 5000 W/m^2 K. Below 1475 °C, h_0 remained constant at 5000 W/m^2 K. These shrink-on h_0 values are up to 100 times greater than the shrink-off values, indicating that it is very important to account for interface geometry/interface pressure in FEM simulations of PMC of Ti-6Al-4V.

The measured *mold* temperature-transient curves were matched reasonably well also (Figure 9). The maximum instantaneous temperature difference between the measured and predicted temperatures in the mold ranged from 20 °C to 100 °C during the initial transient (during which time the effect of pouring and loss of thermocouple contact with the mold would have been greatest) to less than 20 °C thereafter. Hence, the shrink-off $h_0(T)$ curve was deemed applicable to this outer mold-casting interface.

3. *Shrink-on validation*

The shrink-on h_0 results from the trials with the 32-mm-diameter core were applied in a 2-D simulation of the casting trial with the 25-mm-diameter core to test their applicability. The predicted temperature transients showed reasonable agreement with the measured temperature transients from the core thermocouples (Figure 10). The maximum instantaneous temperature difference between the measured and predicted curves at the center of the core was less than 30 °C,

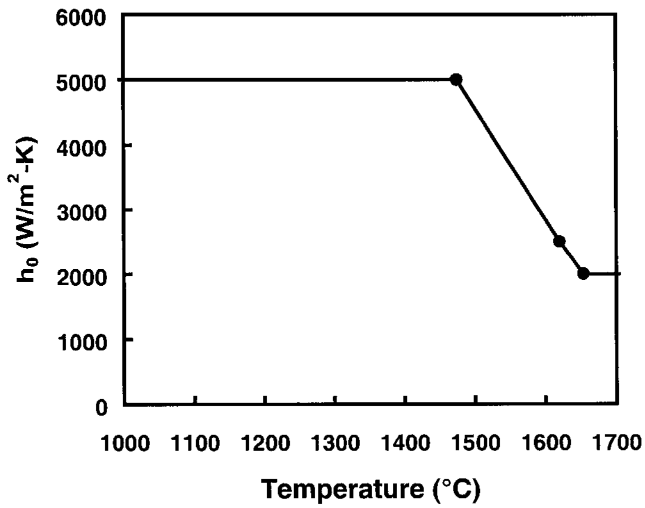

(*a*)

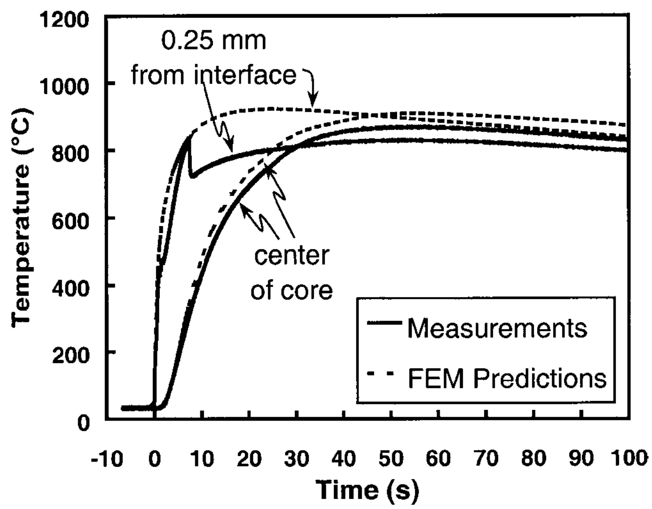

(*b*)

Fig. 8—Calibration-curve results for shrink-on conditions in a casting with a 32-mm-diameter core: (*a*) the $h_0(T)$ curve and (*b*) comparison of measured and FEM-predicted core temperature transients.

and both the initial heating rate and the shape of the predicted near-surface curve matched those of the measured curve. Because the difference between the measured and predicted data was generally within the expected range of pour-to-pour variability (based on data from the 51-mm-diameter mold), the $h_0(T)$ curve from the 32-mm-diameter core was, thus, concluded to be generally applicable in shrink-on situations.

The measured mold temperature-transient curves were matched reasonably well also (Figure 11). The maximum instantaneous temperature difference between the measured and predicted temperatures in the mold ranged from 10 °C to 70 °C during the initial transient (during which time the effect of pouring and loss of thermocouple contact with the mold would have been greatest) to less than 20 °C thereafter. Hence, the shrink-off $h_0(T)$ curve was deemed applicable to this outer mold-casting interface.

C. *Sensitivity Analysis Results*

Thermocouple-measured mold temperatures should in all cases be lower than or equal to actual mold temperatures

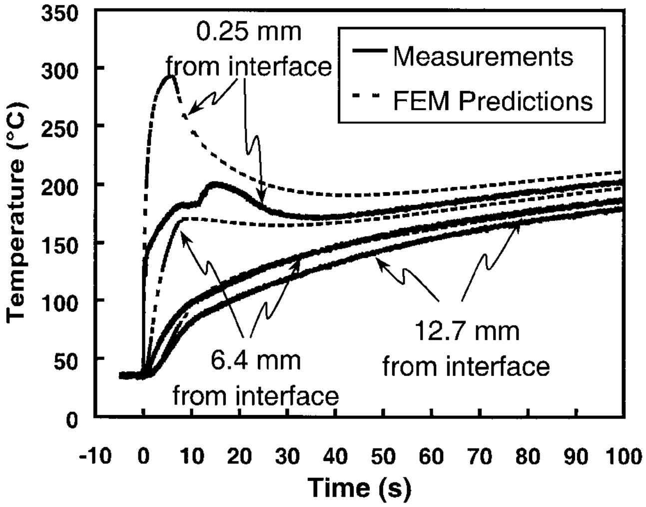

Fig. 9—Comparison of measured mold temperatures for three thermocouple locations and FEM predictions using the $h_0(T)$ curve in Fig. 5(a) for the *outer* mold-casting interface for casting into a 57-mm-diameter mold with a 32-mm-diameter core.

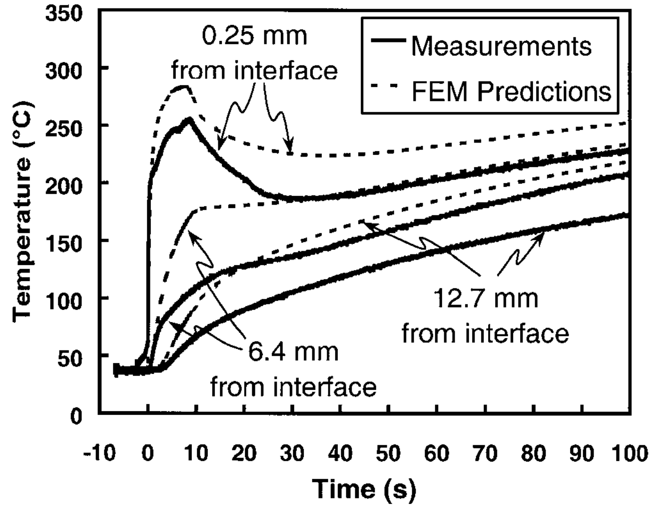

Fig. 11—Comparison of measured mold temperatures for three thermocouple locations and those predicted by an FEM simulation using the $h_0(T)$ curve in Fig. 5(a) for the outer mold-casting interface for casting into a 57-mm-diameter mold with a 25-mm-diameter core.

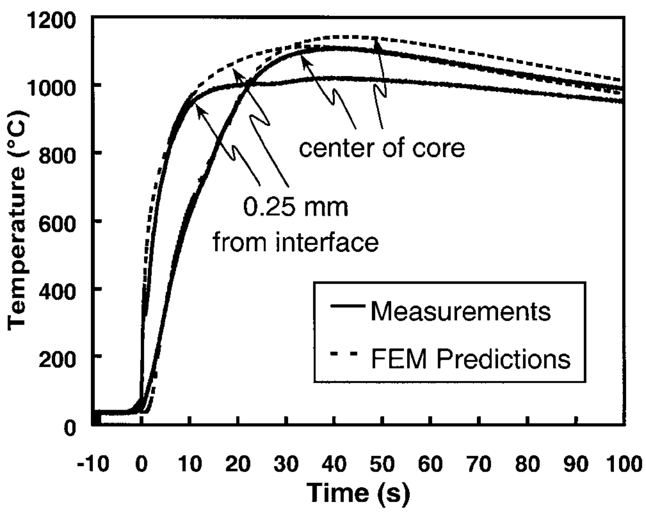

Fig. 10—Comparison of average measured core temperatures for two thermocouple locations and those predicted by an FEM simulation using the $h_0(T)$ curve in Fig. 8(a) for the core-casting interface for casting into a 57-mm-diameter mold with a 25-mm-diameter core.

due to the finite heat-transfer coefficient between the thermocouple and the mold and the possibility that the thermocouples separated from the mold during casting (due to the difference in thermal expansion/contraction). Hence, all of the results presented above represent *lower* bounds for both mold/core temperatures and $h_0(T)$. Unfortunately, it was not possible to estimate the error in the measured temperatures accurately. Hence, a sensitivity analysis was conducted to assess the impact of such errors on the temperature transients in molds and castings. The results of this analysis are presented in Sections 1 and 2.

1. *Shrink-off casting*

Increasing all of the h_0 values in the shrink-off mold by 50 pct resulted in an increase of up to 40 °C in the predicted mold temperatures (Figure 12(a)). The 50 pct increase also affected the predicted casting temperatures; the predicted cooling rates were higher, resulting in a decrease of up to 30 pct in the predicted solidification times (Figure 12(b)). In contrast, increasing the h_0 values by up to 1000 pct at temperatures equal to or greater than the liquidus temperature caused an increase in the initial heating rate of the mold. Such an increase had a negligible effect on the predicted mold temperatures (at times greater than 2 seconds) *and* the predicted casting temperatures (Figures 12(a) and (b)).

2. *Shrink-on casting*

For the shrink-on casting, increasing all of the h_0 values by 50 pct resulted in an *initial* increase of up to 150 °C in the predicted core temperatures followed by a *decrease* of up to 50 °C (Figure 12(c)). The corresponding outer-mold temperatures were up to 25 °C higher (Figure 12(d)). The predicted cooling rates in the casting were also higher, resulting in a decrease of up to 60 pct in the predicted solidification times (Figure 12(e)). Increasing the h_0 values by up to 1000 pct at temperatures equal to or greater than the liquidus temperature caused an increase in the initial heating rate of the core and the outer mold. Such an increase had a negligible effect on both the predicted core and outer-mold temperatures (at times greater than 2 seconds) *and* the predicted casting temperatures (Figures 12(c) through (e)). Increasing the final shrink-on h_0 value by up to 1000 pct caused an increase in the predicted core heating rates, an increase of up to 80 °C in the peak core temperatures, and a decrease of up to 20 °C in the predicted outer-mold temperatures (Figures 12(c) and (d)). This increase affected the predicted casting temperatures in an interesting manner. The predicted temperatures near the outer-mold surface were unaltered, while the temperatures near the core surface and at the center of the casting were significantly decreased, and the resulting solidification times reduced by up to 50 pct (Figure 12(e)).

Based on these results, it was concluded that the FEM simulation results *are not* sensitive to increases in the value

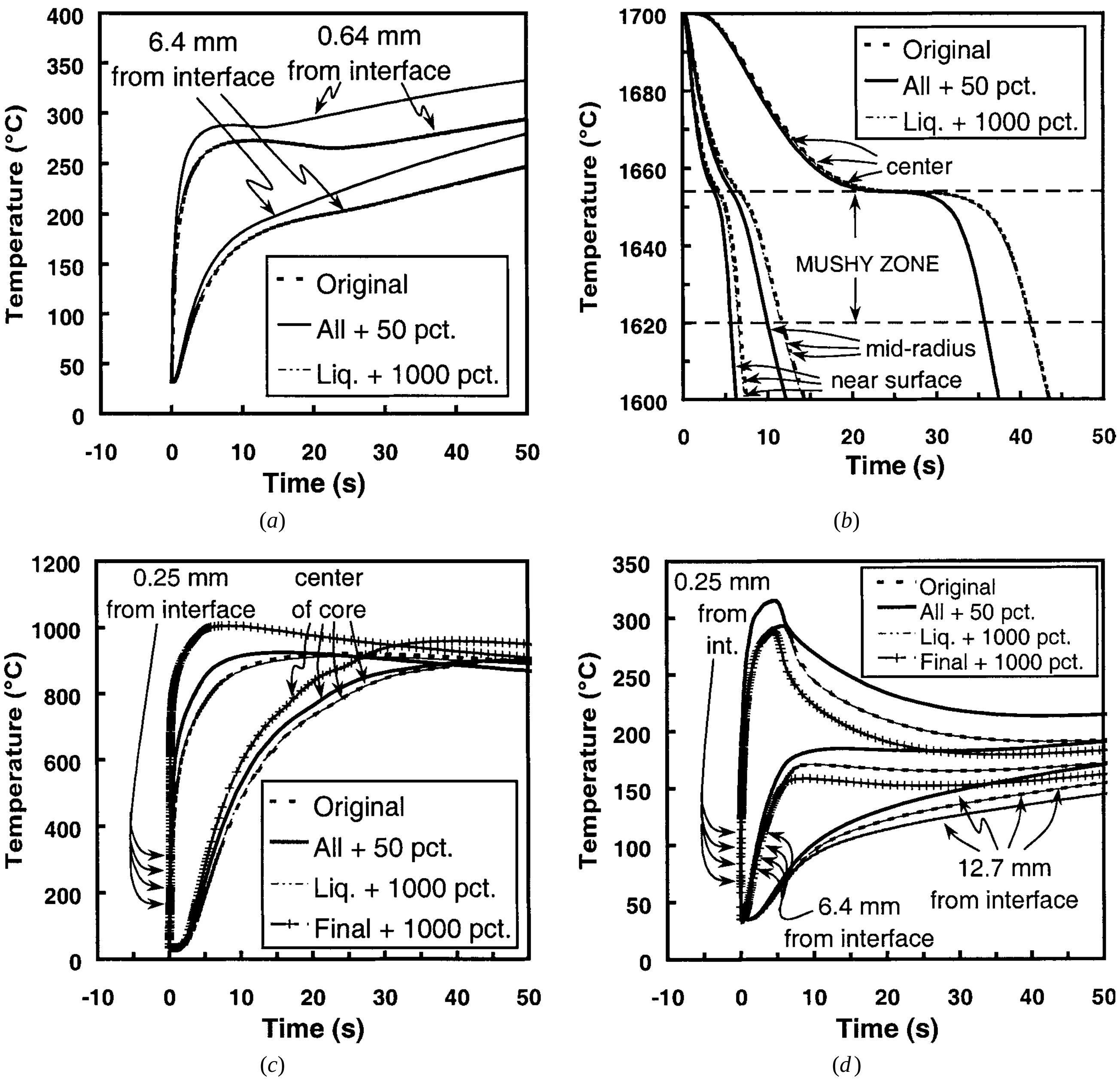

Fig. 12—Comparison of FEM-predicted temperatures for various $h_0(T)$ curves: (*a*) shrink-off mold temperatures, (*b*) shrink-off casting temperatures, (*c*) shrink-on-core temperatures, (*d*) shrink-on outer-mold temperatures, and (*e*) shrink-on casting temperatures.

of h_0 at temperatures above the liquidus temperature but *are* sensitive to increases in the value of h_0 at lower temperatures. Hence, if the actual mold and core temperatures were significantly higher than the measured mold temperatures, the actual heat-transfer coefficients could also be higher than those determined here. However, based on the sensitivity analysis results, the h_0 values reported here are likely of the correct order of magnitude.

D. *Comparison to Literature Results for Casting of Aluminum*

The h_0 values determined here for Ti-6Al-4V were compared to published values for 34-mm-diameter, 75-mm-tall cylindrical castings of pure aluminum and Al-13.2Si (Figure 13(a)) and 90-mm-inner-diameter, 120-mm-outer-diameter, 60-mm-tall pipe-shaped castings of pure aluminum, Al-12.6Si, and alloys AC8A and A356 (Figures 13(b) and (c)). To facilitate this comparison, $h_0(t)$ curves were extracted from the 2-D axisymmetric simulation results for the Ti-6Al-4V castings. There were two major differences between the titanium and aluminum $h_0(t)$ curves.

(1) Because pouring was not simulated and h_0 was specified as a function of temperature, there was no initial increase in h_0 with time for the titanium casting simulation results.
(2) Because titanium has a much higher melting point than aluminum, it solidifies faster and, correspondingly, changes in h_0 occur earlier.

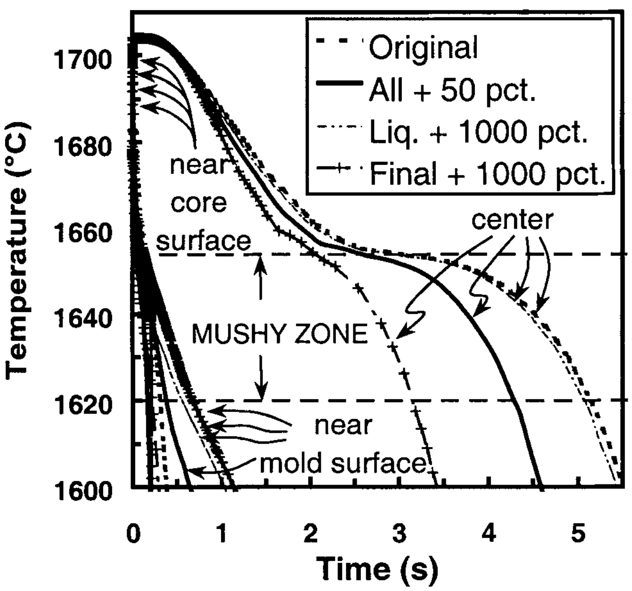

(*e*)

Fig. 12—Continued. Comparison of FEM-predicted temperatures for various $h_0(T)$ curves: (*a*) shrink-off mold temperatures, (*b*) shrink-off casting temperatures, (*c*) shrink-on-core temperatures, (*d*) shrink-on outer-mold temperatures, and (*e*) shrink-on casting temperatures.

Aside from these expected differences, the shapes of the $h_0(t)$ curves for titanium and aluminum were similar. However, there were several other differences. For the shrink-off castings (Figures 13(a) and (b)), the peak value for titanium was 30 to 40 pct lower than the peaks for aluminum. However, based on the sensitivity analysis results, this difference would have led to a relatively small change in the solidification rate of the casting. For the shrink-on casting, the shrink-on h_0 for titanium reached a steady-state maximum value, while for aluminum, h_0 continued to increase with time. One possible explanation for this difference can be deduced based on the results of Semiatin *et al.*[9] and Hu *et al.*[10] which showed that h_0 reaches a steady-state maximum at a critical value of applied pressure. It is possible that the interface pressure did not reach the critical value in the aluminum castings but did in the titanium castings. For instance, differences in the mold geometries and mold temperature transients could have resulted in different interface pressures for the various castings. Additionally, differences in casting-alloy properties, such as mold-surface wetting, solidification type, solidification shrinkage, thermal-expansion coefficient, and deformation characteristics are likely to have caused differences in both the actual interface contact pressure *and* the critical interface pressure. For example, as interface contact pressure increases, the asperities in the harder titanium might stop deforming (resulting in a constant value of h_0), while those in the softer aluminum might continue to deform, resulting in better contact at the interface and, thus, a continued increase in h_0. However, regardless of these differences, the h_0 values for metal-mold casting of titanium were generally similar to those for metal-mold casting of aluminum.

IV. SUMMARY AND CONCLUSIONS

Values of the interface heat-transfer coefficient as a function of casting surface temperature and interface contact

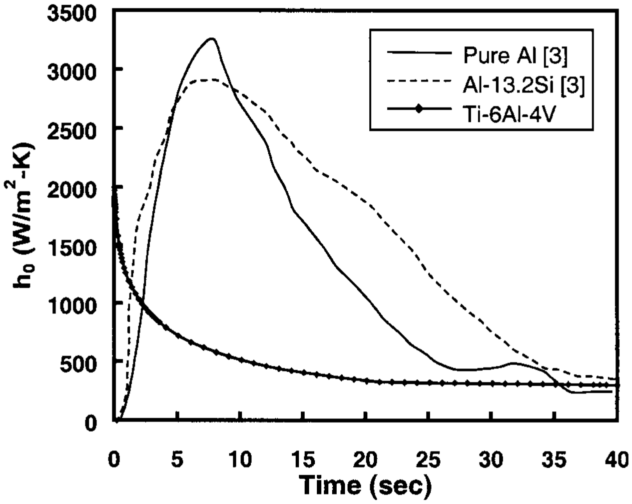

(*a*)

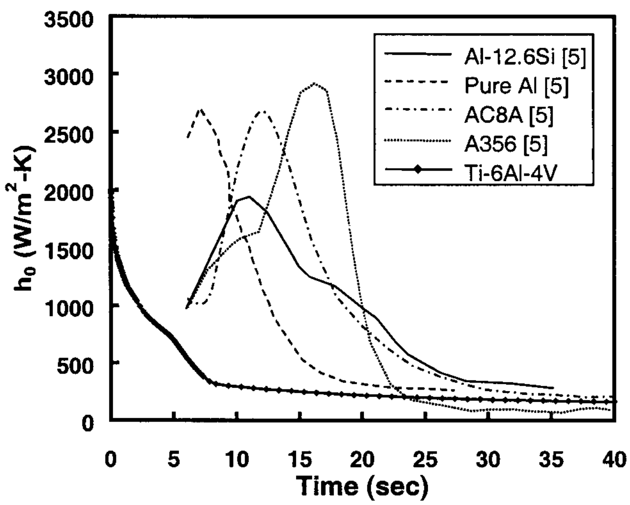

(*b*)

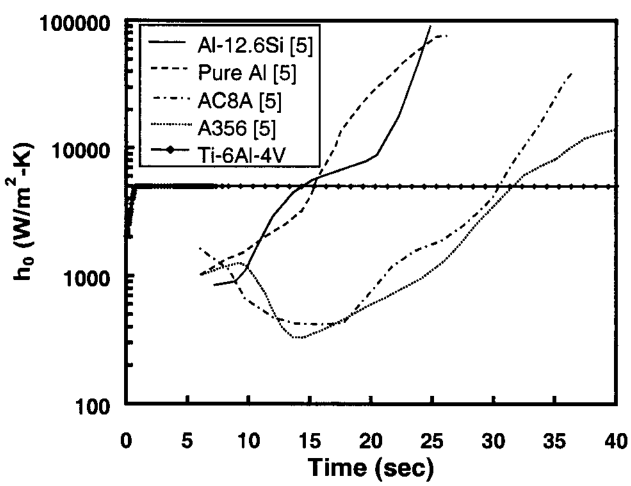

(*c*)

Fig. 13—Comparison of $h_0(t)$ curves for PMC of Ti-6Al-4V (present work) to published $h_0(t)$ curves for various aluminum alloys for (*a*) the mold-casting interface for cylindrical castings, (*b*) the outer mold-casting interface, and (*c*) the core-casting interface for tube-shaped castings.

condition were established for PMC of Ti-6Al-4V using a calibration-curve method. Values of h_0 were determined for two limiting interface types, shrink-off and shrink-on, based on thermocouple data from within the molds. The thermal FEM models were assumed to accurately predict the thermal history of the castings provided that accurate input was used in the simulations. From this work, the following conclusions were drawn.

1. The interface heat-transfer coefficient for PMC of Ti-6Al-4V can be specified as a function of the surface temperature of the casting.
2. The interface type (*i.e.*, shrink-off or shrink-on) can alter the value of h_0 by up to two orders of magnitude. Therefore, interface pressure should be taken into account in FEM simulations.
3. FEM results are not sensitive to increases in h_0 at or above the liquidus temperature, but are sensitive to increases in h_0 at lower temperatures.
4. The values of h_0 for permanent-mold casting of Ti-6Al-4V are generally similar to those reported in the literature for metal-mold casting of aluminum alloys.

ACKNOWLEDGMENTS

This work was conducted as part of the in-house research activities of the Processing Science Group, Air Force Research Laboratory, Materials and Manufacturing Directorate. The support and encouragement of the Laboratory management and the Air Force Office of Scientific Research (Dr. S. Wu, program manager) and the assistance provided by Howmet Research Corporation personnel are gratefully acknowledged. Technical discussions with R. Shivpuri and C. Mobley and the assistance of D. Barker, T. Brown, J. Brown, P. Fagin, and T. Goff in performing the experimental work are also greatly appreciated.

REFERENCES

1. G.N. Colvin: *Titanium '95*, P.A. Blenkinsop, W.J. Evans, and H.N. Flower, eds., Institute of Materials, London, 1996, pp. 691-701.
2. J. Papai and C. Mobley: Report No. ERC/NSM-887-13, Engineering Research Center for Net Shape Manufacturing, Columbus, OH, 1987.
3. Y. Nishida and H. Matsubara: *Br. Foundryman*, 1976, vol. 69, pp. 274-78.
4. Y. Nishida, W. Droste, and S. Engler: *Metall. Trans. B*, 1986, vol. 17B, pp. 833-44.
5. L.J.D. Sully: *AFS Trans.*, 1976, vol. 84, pp. 735-44.
6. T.-G. Kim and Z.-H. Lee: *Int. J. Heat Mass Transfer*, 1997, vol. 40 (15), pp. 3513-25.
7. P.A. Kobryn and S.L. Semiatin: AFRL Materials & Manufacturing Directorate, WPAFB, OH, unpublished research, 1999.
8. K. Ho and R.D. Pehlke: *AFS Trans.*, 1984, vol. 61, pp. 587-98.
9. S.L. Semiatin, E.W. Collings, V.E. Wood, and T. Altan: *J. Eng. Industry*, 1987, vol. 109, pp. 49-57.
10. Z.M. Hu, J.W. Brooks, and T.A. Dean: *Proc Inst. Mech Eng.*, 1998, vol. 212, part C, pp. 485-96.
11. *ProCAST™ Users Manual & Technical Reference*, Version 3.1.0, UES Software, Inc., Dayton, OH, 1998.
12. J.B. Henderson and H. Groot: Technical Report No. TPRL 1284, Thermophysical Properties Research Laboratory, Purdue University, West Lafayette, IN, 1993.
13. H. Groot, J. Ferrier, and D.L. Taylor: Technical Report No. TPRL 1728, Thermophysical Properties Research Laboratory, Purdue University, West Lafayette, IN, 1996.